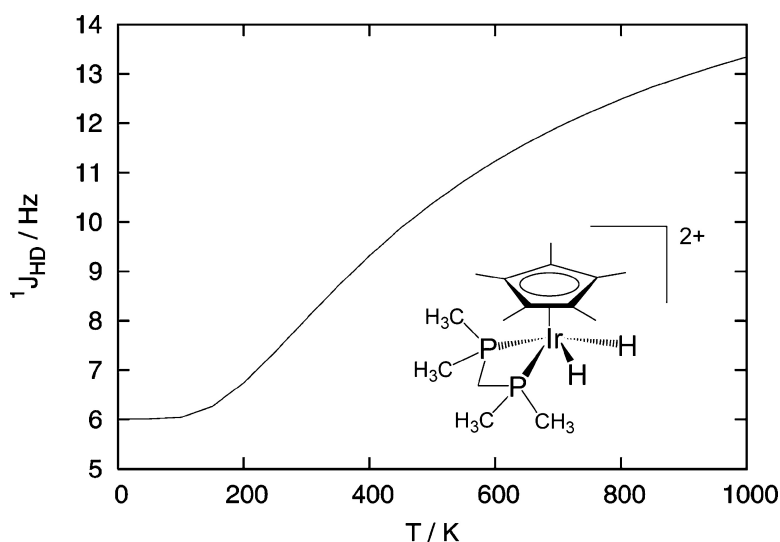


Determination of the Temperature Dependence of the H–D Spin–Spin Coupling Constant and the Isotope Effect on the Proton Chemical Shift for the Compressed Dihydride Complex [Cp*Ir(P–P)H]

Ricard Gelabert, Miquel Moreno, Jos M. Lluch, Agust Lleds, and D. Michael Heinekey

J. Am. Chem. Soc., **2005**, 127 (15), 5632-5640 • DOI: 10.1021/ja043011r • Publication Date (Web): 24 March 2005

Downloaded from <http://pubs.acs.org> on March 25, 2009



More About This Article

Additional resources and features associated with this article are available within the HTML version:

- Supporting Information
- Links to the 3 articles that cite this article, as of the time of this article download
- Access to high resolution figures
- Links to articles and content related to this article
- Copyright permission to reproduce figures and/or text from this article

[View the Full Text HTML](#)

Determination of the Temperature Dependence of the H–D Spin–Spin Coupling Constant and the Isotope Effect on the Proton Chemical Shift for the Compressed Dihydride Complex $[\text{Cp}^*\text{Ir}(\text{P}–\text{P})\text{H}_2]^{2+}$

Ricard Gelabert,[†] Miquel Moreno,[†] José M. Lluch,^{*,†} Agustí Lledós,[†] and D. Michael Heinekey[‡]

Contribution from the Departament de Química, Universitat Autònoma de Barcelona, 08193 Bellaterra, Barcelona, Spain, and Department of Chemistry, Box 351700, University of Washington, Seattle, Washington 98195-1700

Received November 19, 2004; E-mail: lluch@klingson.uab.es

Abstract: Complex $[\text{Cp}^*\text{Ir}(\text{dmpm})\text{H}_2]^{2+}$ (dmpm = bis(dimethylphosphino)methane) has been reported to display temperature-dependent spin–spin coupling constant ($^1J_{\text{HD}}$) and isotope effect on the ^1H NMR chemical shift ($\Delta\delta$). A combined electronic structure density functional theory + quantum nuclear dynamics study is used to determine from first-principles the unusual temperature dependence of the spin–spin coupling constant. It is found that the potential energy surface describing the motion of the Ir–H₂ unit has a deeper minimum in the dihydride region and is characterized by important anharmonicities. These anomalies affect the nature of the vibrational states of the unit and are the main reason for the unusual temperature dependence of $^1J_{\text{HD}}$ and $\Delta\delta$. These results suggest experimental tests to identify compressed dihydride transition metal complexes.

1. Introduction

In the 20 years since Kubas characterized the first dihydrogen complex,¹ these complexes and transition metal hydrides in general have been the subject of intensive investigation. Productive synergies between experimental and theoretical studies have led to an increased understanding of the binding and activation of hydrogen by transition metal centers.² This area of investigation has been reviewed several times,^{3,4} most comprehensively by Kubas.⁵

A key aspect of the structure of these complexes is the H–H distance ($R_{\text{H–H}}$), which has been found to be in the range 0.8–1.0 Å in the vast majority of complexes reported to date. In contrast, conventional dihydride and polyhydride complexes have $R_{\text{H–H}} \geq 1.5$ Å.⁶ However, a modest but increasing number of species where the H–H distance falls between these limits is now known. Such complexes have been termed “stretched” or “elongated” dihydrogen complexes.⁷ It is reasonable to see both dihydrogen and dihydride complexes as just extreme cases of a single type of complex with a hydrogen molecule bound

to the metal. The structure adopted depends on a subtle balance between donation from the occupied bonding orbital of the H₂ molecule and back-donation to the σ^* orbital. All of these complexes show intriguing quantum mechanical properties, owing to the lightness of the atoms involved. These include quantum exchange processes in dihydride transition metal complexes, rotational tunneling in dihydrogen complexes,^{8,9} and extensive hydrogen delocalization in the case of stretched dihydrogen complexes.^{10,11}

Direct experimental measurement of $R_{\text{H–H}}$ is difficult. X-ray diffraction is not definitive, and relatively few complexes have proven amenable to neutron diffraction experiments. Solid-state NMR measurement of $R_{\text{H–H}}$ for some dihydrogen complexes from dipolar couplings has been reported, but the majority of $R_{\text{H–H}}$ values have relied upon indirect methods. Estimates of $R_{\text{H–H}}$ for some dihydrogen complexes have been reported based on $T_{1(\text{min})}$ measurements,¹² but the most convenient method for determining $R_{\text{H–H}}$ uses measurement of $^1J_{\text{HD}}$ in partially deuterated derivatives. This method is based on the inverse relationship between $R_{\text{H–H}}$ and $^1J_{\text{HD}}$, which was first established empirically.^{13,14} This approach was later put on sounder

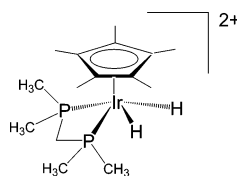
[†] Universitat Autònoma de Barcelona.

[‡] University of Washington.

(1) Kubas, G. J.; Ryan, R. R.; Swanson, B. I.; Vergamini, P. J.; Wasserman, H. J. *J. Am. Chem. Soc.* **1984**, *106*, 451–452.
 (2) Maseras, F.; Lledós, A.; Clot, E.; Eisenstein, O. *Chem. Rev.* **2000**, *100*, 601–636.
 (3) Heinekey, D. M.; Oldham, W. J., Jr. *Chem. Rev.* **1993**, *93*, 913–926.
 (4) Morris, R. H.; Jessop, P. G. *Coord. Chem. Rev.* **1992**, *121*, 155–289.
 (5) Kubas, G. J. *Metal Dihydrogen and σ -Bond Complexes: Structure, Theory and Reactivity*; Kluwer: New York, 2001.
 (6) McGrady, G. S.; Guilera, G. *Chem. Soc. Rev.* **2003**, *32*, 383–392.
 (7) Heinekey, D. M.; Lledós, A.; Lluch, J. M. *Chem. Soc. Rev.* **2004**, *33*, 175–182.

(8) Gelabert, R.; Moreno, M.; Lluch, J. M.; Lledós, A. *Organometallics* **1997**, *16*, 3805–3814.
 (9) Eckert, J.; Webster, C. E.; Hall, M. B.; Albinati, A.; Venanzi, L. M. *Inorg. Chim. Acta* **2002**, *330*, 240–249.
 (10) Gelabert, R.; Moreno, M.; Lluch, J. M.; Lledós, A. *J. Am. Chem. Soc.* **1997**, *119*, 9840–9847.
 (11) Gelabert, R.; Moreno, M.; Lluch, J. M.; Lledós, A. *J. Am. Chem. Soc.* **1998**, *120*, 8168–8176.
 (12) Desrosiers, P. J.; Cai, L.; Lin, Z.; Richards, R.; Halpern, J. *J. Am. Chem. Soc.* **1991**, *113*, 4173–4184.
 (13) Heinekey, D. M.; Luther, T. A. *Inorg. Chem.* **1996**, *35*, 4396–4399.

Chart 1



theoretical grounds by Hush¹⁵ and finally by Limbach and Chaudret.¹⁶ Recently the Limbach/Chaudret correlation has been slightly reworked by us.¹⁷

The reliability of the indirect measurement of R_{H-H} through $^1J_{HD}$ coupling constants was cast into doubt when the case of the elongated dihydrogen complexes and compressed dihydride complexes was considered.¹⁷ These complexes display measurable temperature dependence of $^1J_{HD}$, a characteristic not seen in normal dihydrogen or dihydride complexes.^{14,18,19} For instance, the elongated dihydrogen complex $[Cp^*Ru(dppm)(H_2)]^+$ (**1**) (dppm = bis(diphenylphosphino) methane) with $R_{H-H} = 1.10$ Å determined by neutron diffraction displays decreasing $^1J_{HD}$ with temperature: 22.3 ± 0.2 Hz at 213 K and 21.1 ± 0.2 Hz at 295 K.¹⁸ In a theoretical study of a modeled version of complex **1**, which included quantum dynamics treatment of the motion of the dihydrogen ligand, high anharmonicity was found in the part of the potential energy surface describing the motion of the $M-H_2$ unit of the complex. Together with the varying population of excited vibrational states of the $M-H_2$ unit as a function of temperature, this was used to explain the observed behavior in terms of lengthening of R_{H-H} .¹⁰ This study also predicted a structural isotope effect, which was later confirmed experimentally.^{20,21}

A similar treatment was carried out on a model of complex $trans-[Os(H_2)(dppe)_2Cl]^+$ (dppe = 1,2-bis(diphenylphosphino)ethane) ($R_{H-H} = 1.22$ Å, neutron diffraction data),¹¹ and very recently a quantum dynamics treatment has been applied to $[Cp^*Ir(dmpm)H_2]^{2+}$ (**2**) (dmpm = bis(dimethylphosphino) methane),¹⁷ depicted in Chart 1. Both systems show the opposite experimental behavior: $^1J_{HD}$ increases with temperature. The temperature dependence of $^1J_{HD}$ was explained by a simplified electronic structure + nuclear dynamics study in the same methodological terms as for complex **1**,¹⁰ except that **2** was found to have a stable minimum in the dihydride region, which led to use of the term “compressed dihydride” rather than “elongated dihydrogen” to describe the structure. For this complex **2** a decrease of R_{H-H} with temperature would cause the observed $^1J_{HD}$ behavior.

To date, the temperature dependence of $^1J_{HD}$ in the stretched dihydrogen complexes has been rationalized indirectly via the temperature dependence of R_{H-H} . The advent of powerful computers and sophisticated algorithms has made it possible to

compute NMR chemical shifts and spin–spin coupling constants directly. Theoretical studies have been appearing in the literature that report very different problems through theoretically computed spin–spin coupling constants: complexes of metal dications and nucleic acid bases,²² spin–spin coupling across hydrogen bonds in proteins,²³ determination of π -character of C–C bonds in small organic molecules,²⁴ and spin–spin coupling constants involving heavy atoms in transition metal complexes.^{25,26} Computations of spin–spin coupling constant *surfaces* have been reported (i.e., determination of their value for a range of continuously distorted geometries of a molecule).^{27,28}

Even though some authors have shown that $^1J_{H-D}$ can be accurately calculated for a range of dihydride and dihydrogen complexes,²⁹ including elongated dihydrogen complexes,³⁰ no attempt has been made to explain from first-principles the temperature dependence of $^1J_{HD}$ for elongated dihydrogen or compressed dihydride complexes *directly*, that is, without using a certain correlation between R_{H-H} and $^1J_{HD}$. In this article, we carry out a comprehensive electronic structure study of complex **2** in which $^1J_{HD}$ and δ surfaces are determined. A 2D nuclear dynamics study is done on the complex, including an anharmonic vibrational analysis of the $Ir-H_2$ unit, and the results combined to reproduce the temperature dependence of $^1J_{HD}$ and the isotope effect on the chemical shift, $\Delta\delta$.

2. Computational Details

2.1. Electronic Structure Calculations. No modeling has been done on complex **2** in any calculations. The only restriction imposed has been global C_s symmetry, which has been adopted for computational efficiency. The *Gaussian 03* program has been used in all electronic structure calculations.³¹ Electronic structure calculations have been done at the density functional theory (DFT) level.^{32,33} The functional chosen is the three-parameter hybrid functional of Becke, and the Lee, Yang, and Parr correlation functional, widely known as B3LYP.^{34,35} An

- (14) Maltby, P. A.; Schlaf, M.; Steinbeck, M.; Lough, A. J.; Morris, R. H.; Klooster, W. T.; Koetzle, T. F.; Srivastava, R. C. *J. Am. Chem. Soc.* **1996**, *118*, 5396–5407.
- (15) Hush, N. S. *J. Am. Chem. Soc.* **1997**, *119*, 1717–1719.
- (16) Gründemann, S.; Limbach, H. H.; Buntkowsky, G.; Sabo-Etienne, S.; Chaudret, B. *J. Phys. Chem. A* **1999**, *103*, 4752–4754.
- (17) Gelabert, R.; Moreno, M.; Lluch, J. M.; Lledós, A.; Pons, V.; Heinekey, D. M. *J. Am. Chem. Soc.* **2004**, *126*, 8813–8822.
- (18) Klooster, W. T.; Koetzle, T. F.; Jia, G. C.; Fong, T. P.; Morris, R. H.; Albinati, A. *J. Am. Chem. Soc.* **1994**, *116*, 7677–7681.
- (19) Pons, V.; Heinekey, D. M. *J. Am. Chem. Soc.* **2003**, *125*, 8428–8429.
- (20) Law, J. K.; Mellows, H.; Heinekey, D. M. *J. Am. Chem. Soc.* **2001**, *123*, 2085–2086.
- (21) Law, J. K.; Mellows, H.; Heinekey, D. M. *J. Am. Chem. Soc.* **2002**, *124*, 1024–1030.

- (22) Sychrovsky, V.; Sponer, J.; Hobza, P. *J. Am. Chem. Soc.* **2004**, *126*, 663–672.
- (23) Tuttle, T.; Kraka, E.; Wu, A. A.; Cremer, D. *J. Am. Chem. Soc.* **2004**, *126*, 5093–5107.
- (24) Gräfenstein, J.; Kraka, E.; Cremer, D. *J. Phys. Chem. A* **2004**, *108*, 4520–4535.
- (25) Autschbach, J.; Ziegler, T. *J. Am. Chem. Soc.* **2001**, *123*, 5320–5324.
- (26) Autschbach, J.; Le Guennic, B. *J. Am. Chem. Soc.* **2003**, *125*, 13585–13593.
- (27) Delbene, J. E.; Elguero, J.; Alkorta, I.; Yáñez, M.; Mó, O. *J. Chem. Phys.* **2004**, *120*, 3237–3243.
- (28) Ratajczyk, T.; Pecul, M.; Sadlej, J.; Helgaker, T. *J. Phys. Chem. A* **2004**, *108*, 2758–2769.
- (29) Bacsay, G. B.; Bytheway, I.; Hush, N. S. *J. Am. Chem. Soc.* **1996**, *118*, 3753–3756.
- (30) Gusev, D. G. *J. Am. Chem. Soc.* **2004**, *126*, 14249–14257.
- (31) Frisch, M. J.; Trucks, G. W.; Schlegel, H. B.; Scuseria, G. E.; Robb, M. A.; Cheeseman, J. R.; Montgomery, J. A., Jr.; Vreven, T.; Kudin, K. N.; Burant, J. C.; Millam, J. M.; Iyengar, S. S.; Tomasi, J.; Barone, V.; Mennucci, B.; Cossi, M.; Scalmani, G.; Rega, N.; Petersson, G. A.; Nakatsuji, H.; Hada, M.; Ehara, M.; Toyota, K.; Fukuda, K.; Hasegawa, J.; Ishida, M.; Nakajima, T.; Honda, Y.; Kitao, O.; Nakai, H.; Klene, M.; Li, X.; Knox, J. E.; Hratchian, H. P.; Cross, J. B.; Adamo, C.; Jaramillo, J.; Gomperts, R.; Stratmann, R. E.; Yazyev, O.; Austin, A. J.; Cammi, R.; Pomelli, C.; Ochterski, J. W.; Ayala, P. Y.; Morokuma, K.; Voth, G. A.; Salvador, P.; Dannenberg, J. J.; Zakrzewski, V. G.; Dapprich, S.; Daniels, A. D.; Strain, M. C.; Farkas, O.; Malick, D. K.; Rabuck, A. D.; Raghavachari, K.; Foresman, J. B.; Ortiz, J. V.; Cui, Q.; Baboul, A. G.; Clifford, S.; Cioslowski, J.; Stefanov, B. B.; Liu, G.; Liashenko, A.; Piskorz, P.; Komaromi, I.; Martin, R. L.; Fox, D. J.; Keith, T.; Al-Laham, M. A.; Peng, C. Y.; Nanayakkara, A.; Challacombe, M.; Gill, P. M. W.; Johnson, B.; Chen, W.; Wong, M. W.; Gonzalez, C.; Pople, J. A. *Gaussian 03*, Revision B.04; Gaussian, Inc.: Pittsburgh, PA, 2003.
- (32) Parr, R. G.; Yang, W. *Density Functional Theory of Atoms and Molecules*; Oxford University Press: Oxford, U.K., 1989.
- (33) Ziegler, T. *Chem. Rev.* **1991**, *91*, 651–667.
- (34) Lee, C. T.; Yang, W. T.; Parr, R. G. *Phys. Rev. B* **1988**, *37*, 785–789.
- (35) Becke, A. D. *J. Chem. Phys.* **1993**, *98*, 5648–5652.

effective core operator has been used to replace the core electrons of the iridium atom.³⁶ Its outer electrons have been described with the basis set associated with the pseudopotential of Hay and Wadt with a standard double- ξ LANL2DZ contraction.^{31,36} The phosphorus atoms have been described with the same pseudopotential and basis set, enlarged with d polarization functions.³⁷ The standard split-valence 6-31G basis set was used for the rest of the atoms,³⁸ except the five carbon atoms comprising the cyclopentadienyl ring and that bridging the phosphorus atoms, for which the 6-31G(d) basis set has been chosen.³⁹ For the H atoms bound to Ir, the 6-31G(p) basis set has been selected.⁴⁰

Chemical shifts (δ) relative to hydrogen atoms in tetramethylsilane (TMS) have been obtained from nuclear magnetic shielding tensors computed at the DFT level with the B3LYP functional and using the gauge-invariant atomic orbital (GIAO) method.^{31,41–43} Indirect NMR spin–spin coupling constants for H and D in the HD complex, $^1J_{\text{HD}}$, have been determined at the DFT level using the B3LYP functional and the GIAO method.^{31,44–46} The coupling constants have been computed as a sum of the Fermi contact (FC), spin dipolar (SD), paramagnetic spin–orbit (PSO), and diamagnetic spin–orbit (DSO) contributions. In selected cases, chemical shifts and $^1J_{\text{HD}}$ coupling constants have been computed for structures in which the hydrogen atoms bound to the iridium atom were described with the IGLO-III basis set.⁴⁷

2.2. Nuclear Dynamics Calculations. This study is concerned with the dynamics of the Ir–H₂ unit, and because of the lightness of the hydrogen atoms, a quantum treatment is in order. To determine both energy levels and wave functions of the nuclear motion, the nuclear Schrödinger equation has to be solved:

$$[\hat{T}_{\text{nuclear}} + U(\mathbf{R})]\Psi_{\text{nuclear}} = E\Psi_{\text{nuclear}} \quad (1)$$

where \mathbf{R} is a $3N-6$ component vector describing a given arrangement of the nuclei, and U is the potential energy surface (PES), computed by adding the electronic potential energy plus internuclear repulsion energy obtained within the Born–Oppenheimer approximation (static nuclei). Because computation of the full $U(\mathbf{R})$ is unattainable, a reduction of dimensionality that preserves the main features of the potential energy surface is needed. It has been shown elsewhere that the dynamics of the M–H₂ unit in elongated dihydrogen complexes mixes extensively the H–H and metal–H₂ motions.^{10,11,48} With this in mind, a 2D surface has been computed, the variables chosen being the H–H and Ir–H₂ distances, the latter being defined as the distance between the iridium atom and the point halfway between both hydrogen atoms. This choice renders the kinetic energy operator in eq 1 very simple.

When computing this PES global relaxation of the complex has been allowed, except for the H–H and Ir–H₂ distances while keeping the

complex within C_s symmetry group at all times. A total of nine Ir–H₂ distance values and 11 H–H distance values have been chosen to build a grid of 99 points, each of them corresponding to a DFT calculation. This mesh of points was fitted into a 2D cubic spline functional form to ease further calculations.⁴⁹

To solve eq 1, the discrete variable representation (DVR) method proposed by Colbert and Miller has been chosen.⁵⁰ The DVR representation consisted of a rectangular grid of 20×20 points. After the DVR matrix representation of the Hamiltonian is constructed, its diagonalization yields the eigenvalues (vibrational energy levels) and eigenvectors (vibrational wave functions). The wave functions can be used in further calculations of expectation values and averaged quantities, as will be described in the text. It was verified that results remained essentially invariant upon increasing the number of points in the DVR grid.

3. Results and Discussion

3.1. Static Studies. In a previous study we located several stationary points in the C_s subspace of the global PES, which we summarize here for convenience:¹⁷ it was established that from a purely static point of view (i.e., before nuclear dynamics is considered) complex **2** can be described as a dihydride complex ($R_{\text{H–H}} = 1.63 \text{ \AA}$). Another very shallow minimum describing an elongated dihydrogen structure was found ($R_{\text{H–H}} = 0.93 \text{ \AA}$) higher in potential energy ($U = 1.4 \text{ kcal/mol}$), together with the transition state structure connecting both ($U = 1.7 \text{ kcal/mol}$). The transition state structure for the librational motion of the two hydrogen atoms bound to the iridium atom was found to be high in potential energy ($U = 6.3 \text{ kcal/mol}$), which agrees with complex **2** being described as belonging to a slow rotation regime for this kind of motion.¹⁹

We also showed that a simple 1D quantum dynamical treatment was sufficient to qualitatively describe the geometry of complex **2**, or at least the H–H distance.¹⁷ Such an approach treats simultaneously the H–H and Ir–H₂ motions and underestimates the zero point energy (ZPE). Besides, even though $^1J_{\text{HD}}$ is known to depend on the H–H distance, its dependence on the M–H₂ distance is not known and in principle should not be ignored. The approach used here improves on the previous dynamical treatment, including the H–H and Ir–H₂ degrees of freedom explicitly, and allows for inclusion of anharmonicity in the vibrational study of the Ir–H₂ unit.

The first step is to build the 2D PES, $U(R_{\text{H–H}}, R_{\text{Ir–H}_2})$. This has been done by fixing H–H and Ir–H₂ distances to a range of values and allowing the structure to relax within C_s symmetry. We note that while the C_s dihydrogen structure is a real minimum, the C_s dihydride structure has a small imaginary frequency ($22.6i \text{ cm}^{-1}$) corresponding to the rotation of the Cp* ring. Relaxing the symmetry constraint leads to a C_1 dihydride minimum only $0.07 \text{ kcal mol}^{-1}$ below the C_s dihydride structure in which the Cp* ring has rotated slightly. It is then reasonable to carry out the dynamical study within C_s symmetry. The PES obtained is represented in Figure 1.

As in our previous 2D studies of elongated dihydrogen complexes, the distinguishing feature is the high anharmonicity of the portion of the PES describing the dynamics of the Ir–H₂ unit.^{10,11,48} This was inferred from the preceding 1D study, even though only from a minimum energy pathlike section of the

(36) Hay, P. J.; Wadt, W. R. *J. Chem. Phys.* **1985**, *82*, 299–310.

(37) Hollwarth, A.; Bohme, M.; Dapprich, S.; Ehlers, A. W.; Gobbi, A.; Jonas, V.; Kohler, K. F.; Stegmann, R.; Veldkamp, A.; Frenking, G. *Chem. Phys. Lett.* **1993**, *208*, 237–240.

(38) Hehre, W. J.; Ditchfield, R.; Pople, J. A. *J. Chem. Phys.* **1972**, *56*, 2257–2257.

(39) Francl, M. M.; Pietro, W. J.; Hehre, W. J.; Binkley, J. S.; Gordon, M. S.; Defrees, D. J.; Pople, J. A. *J. Chem. Phys.* **1982**, *77*, 3654–3665.

(40) Hariharan, P. C.; Pople, J. A. *Theor. Chim. Acta* **1973**, *28*, 213–222.

(41) McWeeny, R. *Phys. Rev.* **1962**, *126*, 1028–1028.

(42) Ditchfield, R. *Mol. Phys.* **1974**, *27*, 789–807.

(43) Wolinski, K.; Hinton, J. F.; Pulay, P. *J. Am. Chem. Soc.* **1990**, *112*, 8251–8260.

(44) Barone, V.; Peralta, J. E.; Contreras, R. H.; Snyder, J. P. *J. Phys. Chem. A* **2002**, *106*, 5607–5612.

(45) Sychrovsky, V.; Gräfenstein, J.; Cremer, D. *J. Chem. Phys.* **2000**, *113*, 3530–3547.

(46) Helgaker, T.; Watson, M.; Handy, N. C. *J. Chem. Phys.* **2000**, *113*, 9402–9409.

(47) Kutzelnigg, W.; Fleischer, U.; Schindler, M. *The IGLO-Method: Ab Initio Calculation and Interpretation of NMR Chemical Shifts and Magnetic Susceptibilities*; Springer-Verlag: Heidelberg, 1990; Vol. 23.

(48) Gelabert, R.; Moreno, M.; Lluch, J. M.; Lledós, A. *Chem. Phys.* **1999**, *241*, 155–166.

(49) Press, W. H.; Flannery, B. P.; Teukolsky, S. A.; Vetterling, W. T. *Numerical Recipes in Fortran*, 2nd ed.; Cambridge University Press: Cambridge, U.K., 1992.

(50) Colbert, D. T.; Miller, W. H. *J. Chem. Phys.* **1992**, *96*, 1982–1991.

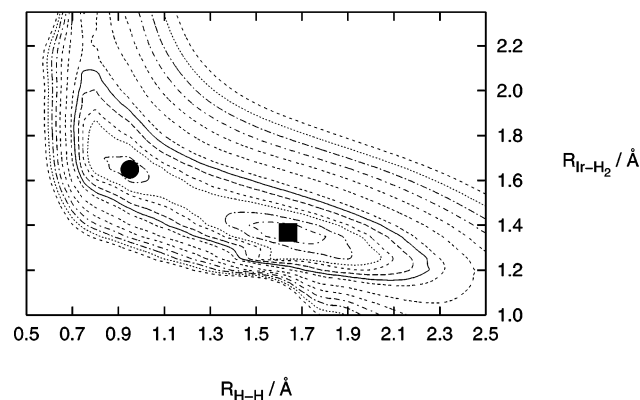


Figure 1. Relaxed potential energy surface of the *cis*-dihydride isomer of complex **2**. Contour lines are: 0.5, 1.5, 3.0, 4.0, 6.0, 8.0, 15.0, 20.0, 25.0, 30.0, 35.0, and 40.0 kcal/mol. Minima on this potential energy surface are denoted with ● (dihydrogen structure) and ■ (*cis*-dihydride structure).

PES. A recent study on the iridium complex $\text{IrH}_3\text{Cl}_2(\text{P}^i\text{Pr}_3)_2$ revealed a very flat potential energy profile with a single minimum in the dihydride region, requiring less than 1 kcal mol^{-1} to change the H–H distance from 1.56 to 1.0 Å.³⁰ Figure 1 reveals the extent to which the H–H bond is disrupted. It is clear that the PES is much narrower in the Ir–H₂ direction than that in the H–H one, and thus if there should be a pure Ir–H₂ stretch, it would be of a higher frequency than that of a hypothetical H–H stretch in the complex.

We turn to the final goal of evaluating the temperature dependence of $^1J_{\text{HD}}$ and proton chemical shift, δ , for which we propose the following procedure. First, we determine the stationary states of a Hamiltonian whose potential energy term is the one just presented (Figure 1) to obtain vibrational energy levels and wave functions. Next, we build a surface by computing $^1J_{\text{HD}}$ for each of the structures on which the potential energy has been computed to build the PES in Figure 1, and we fit this surface into a 2D cubic spline functional form. This surface is actually a function that gives $^1J_{\text{HD}}$ values for specific geometries of the Ir–H₂ unit, $^1J_{\text{HD}}(R_{\text{H}-\text{D}}, R_{\text{Ir}-\text{HD}})$. Then, we can estimate the expectation value of $^1J_{\text{HD}}$ for vibrational state i , $|\chi_i\rangle$, as a vibrational state average of $^1J_{\text{HD}}$:

$$\langle ^1J_{\text{HD}} \rangle_i \approx \frac{\langle \chi_i | ^1J_{\text{HD}}(R_{\text{H}-\text{D}}, R_{\text{Ir}-\text{HD}}) | \chi_i \rangle}{\langle \chi_i | \chi_i \rangle} \quad (2)$$

We note in passing that the PES (Figure 1) is invariant with isotopic composition of the complex. This procedure only involves a series of affordable single point calculations, and we think it is a reasonable approach to evaluate $\langle ^1J_{\text{HD}} \rangle_i$. An analogous procedure is proposed for the state averaged proton chemical shift, $\langle \delta \rangle_i$. This same approach was used with success to compute chemical shifts in low-barrier hydrogen bonds.^{51,52} Proceeding in this way, one would obtain a set of $\langle ^1J_{\text{HD}} \rangle_i$ and $\langle \delta \rangle_i$ values, one per vibrational state, which is the value that would be measured for a system in that vibrational state. To compute the observed value of $^1J_{\text{HD}}$ at a certain temperature T , one should finally compute the Boltzmann average

$$^1J_{\text{HD}}(T) = \frac{1}{Q_0(T)} \sum_i \langle ^1J_{\text{HD}} \rangle_i \exp(-E_i/kT) \quad (3)$$

(and equivalently for $\delta(T)$) where E_i is the vibrational energy of state i relative to the potential energy minimum, and $Q_0(T)$ is the vibrational partition function

$$Q_0(T) = \sum_i \exp(-E_i/kT) \quad (4)$$

Figure 2 shows a contour plot of $^1J_{\text{HD}}(R_{\text{H}-\text{H}}, R_{\text{Ir}-\text{H}_2})$. Some points deserve comment: First, the structure at the potential energy minimum ($R_{\text{H}-\text{H}} = 1.63$ Å, $R_{\text{Ir}-\text{H}_2} = 1.37$ Å) has a $^1J_{\text{HD}}$ value of 5.0 Hz, which is close indeed to the range of $^1J_{\text{HD}}$ values experimentally determined for this complex: 7–9 Hz in the temperature range 223–303 K.¹⁹ Second, the $^1J_{\text{HD}}$ values in the region of configurations describing the dissociation of the complex into $[\text{Cp}^*\text{Ir}(\text{dmpm})]^{2+}$ and HD is slightly more than 40 Hz. Computation of $^1J_{\text{HD}}$ for HD gas with the same basis set and methodology gives a value of $^1J_{\text{HD}} = 51.0$ Hz, which also compares acceptably to the experimental value of $^1J_{\text{HD}}$ for HD gas (43.2 Hz).^{3,53} Finally, on the theoretical determination of $^1J_{\text{HD}}$ in complex $\text{IrH}_3\text{Cl}_2(\text{P}^i\text{Pr}_3)_2$, the value 5.2 Hz was found for two hydride ligands at $R_{\text{H}_2-\text{H}_3} = 1.61$ Å,³⁰ values that compare well to those we have determined. These facts, in our opinion, validate the methodology used to calculate $^1J_{\text{HD}}(R_{\text{H}-\text{H}}, R_{\text{Ir}-\text{H}_2})$ and strengthen our confidence in the ensuing dynamical results on the state averaged spin–spin coupling constant $\langle ^1J_{\text{HD}} \rangle_i$ and its thermal average.

We note that Figure 2 clearly discloses that $^1J_{\text{HD}}$ also depends noticeably on $R_{\text{Ir}-\text{H}_2}$ distances. This gives support to our 2D treatment because we include both $R_{\text{H}-\text{H}}$ and $R_{\text{Ir}-\text{H}_2}$ parameters explicitly and independently in our dynamical approach. Finally, the region of configurational space corresponding to both hydrogen atoms far from the metal and from each other turned out to have very large computed $^1J_{\text{HD}}$ values, possibly an artifact of the methodology. The influence of this in the ensuing calculations is negligible, because of the vanishing amplitude of the vibrational wave functions in this area.

The chemical shift for the H atoms bound to Ir in complex **2** is computed as follows:

$$\delta = \sigma_{\text{TMS}} - \sigma \quad (5)$$

where σ is one-third of the trace of the nuclear magnetic shielding tensor for the hydrogen atoms bound to the metal, and σ_{TMS} is defined as the chemical shift for hydrogen atoms in tetramethylsilane. At our level of calculation, $\sigma_{\text{TMS}} = 31.775$ ppm. The experimental chemical shift reported by Pons and Heinekey is $\delta = -10.48$ ppm for the *cis*-dihydride form of **2** at 298 K.¹⁹ Single point calculations of the nuclear magnetic shielding tensor at the corresponding geometries yield, through use of eq 5, $\delta = -3.93$ ppm for the *cis*-dihydride and $\delta = -2.97$ ppm for the dihydrogen structure. Even though the agreement with experiment is poor, we note that upon increasing temperature, population of vibrational excited states which have higher probability density ($|\psi|^2$) over the dihydrogen region of the PES will likely lead to a displacement of the chemical shift

(51) Garcia-Viloca, M.; Gelabert, R.; González-Lafont, A.; Moreno, M.; Lluch, J. M. *J. Phys. Chem. A* **1997**, *101*, 8727–8733.

(52) Garcia-Viloca, M.; Gelabert, R.; González-Lafont, A.; Moreno, M.; Lluch, J. M. *J. Am. Chem. Soc.* **1998**, *120*, 10203–10209.

(53) Bloyce, P. E.; Rest, A. J.; Whitwell, I.; Graham, W. A. G.; Holmes-Smith, R. *J. Chem. Soc., Chem. Commun.* **1988**, 846–848.

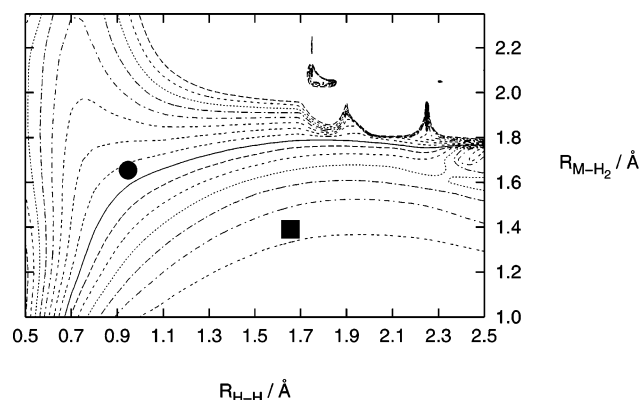


Figure 2. Contour plot of ${}^1J_{\text{HD}}$ as a function of $R_{\text{H-H}}$ and $R_{\text{Ir-H}_2}$. Contours start at 4 Hz (bottom right corner) and increase in 4 Hz intervals. Minima on the potential energy surface are denoted with ● (dihydrogen structure) and ■ (*cis*-dihydride structure).

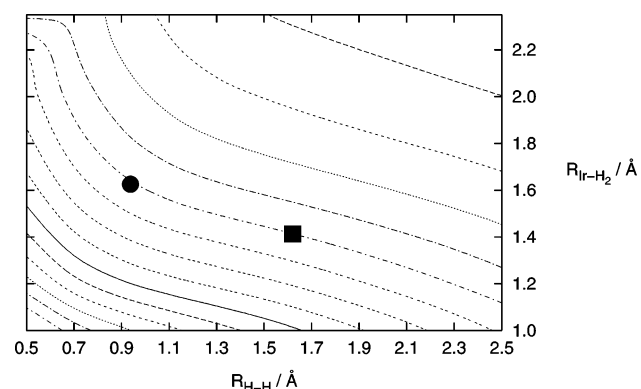


Figure 3. Contour plot of δ as a function of $R_{\text{H-H}}$ and $R_{\text{Ir-H}_2}$. Contours start at -30 ppm (left bottom corner) and increase in 3 ppm intervals. Minima on the potential energy surface are denoted with ● (dihydrogen structure) and ■ (*cis*-dihydride structure).

from the *cis*-dihydride to dihydrogen, that is, to low field, in agreement with experimental findings.¹⁹

The absolute values of the chemical shift are less important than the temperature dependence of the isotope effect on the chemical shift. In a completely analogous way to what has already been discussed for ${}^1J_{\text{HD}}$, a surface for $\delta(R_{\text{H-H}}, R_{\text{Ir-H}_2})$ has been computed and is shown in Figure 3.

It is easy to see that δ also depends on both $R_{\text{Ir-H}_2}$ and $R_{\text{H-H}}$. Moreover, for distances $R_{\text{H-H}} > 1.0$ Å the main dependence is on $R_{\text{Ir-H}_2}$, as can be seen from the fact that, in that region, at constant $R_{\text{H-H}}$ the slope of $\delta(R_{\text{Ir-H}_2})$ is larger than the slope of $\delta(R_{\text{H-H}})$ at constant $R_{\text{Ir-H}_2}$. Besides, δ decreases (i.e., goes to higher field) when $R_{\text{Ir-H}_2}$ decreases. We think that this is very reasonable in view of the conventional interpretation of the relation between δ and electron density (shielding) around a given atom: the shorter $R_{\text{Ir-H}_2}$ is, the closer the hydrogen atoms are to the metal center and thus to its large electron cloud.

It is known that accurate theoretical determination of spin–spin coupling constants and nuclear shielding constants is sensitive to the quality of the basis set. For nuclear shielding constant determination, large basis sets are known to be necessary.⁵⁴ For spin–spin coupling constants, in addition to a large basis set requirement, the dominance of the Fermi-contact contribution makes it necessary, besides, to have a good description of the nuclear region, which in the case of hydrogen

atoms means using $1s$ functions with large exponents.^{54,55} Very good performance has been reported for both nuclear shielding and spin–spin coupling constants with the largest basis sets of Schindler and Kutzelnigg (IGLO basis sets), which are of triple- ζ quality or better.⁴⁷ However, the dynamical nature of this study requires the computation of δ and ${}^1J_{\text{HD}}$ for a large number of structures, which would be very costly with such basis sets. Instead, to validate the δ and ${}^1J_{\text{HD}}$ surfaces we have computed thus far, we have calculated these magnitudes for selected structures of complex **2** where the hydrogen atoms bound to the metal are described with the IGLO-III basis set.

The improved description of the hydrogen atoms with the IGLO-III basis has not changed substantially the ${}^1\text{H}$ chemical shifts for the hydrogen atoms bound to the metal: the hydrogen atoms in the *cis*-dihydride structure appear at -3.70 ppm (compare to -3.93 ppm with 6-31G(p) basis set) and in the dihydrogen structure at -3.14 ppm (compare to -2.97 ppm with 6-31G(p) basis set). We have also computed the value of the chemical shift for free H_2 , which turns out to be $+4.97$ ppm (compare to $+4.90$ with 6-31G(p) basis set). Similarly, we have computed the ${}^1J_{\text{HD}}$ coupling constant for the same structures using the IGLO-III basis set for the hydrogen atoms bound to the metal: for the *cis*-dihydride ${}^1J_{\text{HD}} = 5.4$ Hz (to be compared to 5.0 Hz with 6-31G(p) basis set), for the dihydrogen structure ${}^1J_{\text{HD}} = 30.6$ Hz (compare to 30.8 Hz, computed with the 6-31G(p) basis set), and for free HD ${}^1J_{\text{HD}} = 42.8$ Hz (compare to 51.0 Hz with 6-31G(p) basis set). These results show that the ${}^1\text{H}$ chemical shift and the ${}^1J_{\text{HD}}$ surfaces computed with the smaller basis set are adequate for the purposes of this work.

3.2. Dynamical Studies. The 2D potential energy surface computed above reveals that the potential energy profile for the motion of the Ir– H_2 unit is very anharmonic and the H–H and Ir– H_2 motions are extensively mixed. This hardly comes as a surprise, as it seems to be the norm rather than the exception for the family of elongated dihydrogen complexes, as was suggested for a while and actually verified in theoretical studies.^{10,11,48} In this and similar systems, no single point in the potential energy surface can be considered as “representative” of the geometry of the complex. Rather, the light mass of the H_2 ligand ensures a substantial ZPE for the vibrational motion of the M– H_2 unit. This, together with the impressive anharmonicity in this potential energy surface describing the same motion, causes the vibrational wave function for the ground state to have non-negligible amplitude over large areas of configurational space. In such case, a quantum dynamical treatment of the motion of the M– H_2 unit is indispensable.

To determine vibrational energy levels and wave functions, eq 1 has to be solved. The potential energy surface computed in the previous section (Figure 1) will be used for $U(\mathbf{R})$. This potential energy surface has been built in terms of the $R_{\text{H-H}}$ and $R_{\text{Ir-H}_2}$ variables. Because of the definition of both coordinates, these are orthogonal and the kinetic energy term of the Hamiltonian is simple

$$\hat{T}_{\text{nuclear}} = -\frac{1}{2\mu_{\text{H-H}}} \frac{\partial^2}{\partial R_{\text{H-H}}^2} - \frac{1}{2\mu_{\text{Ir-H}_2}} \frac{\partial^2}{\partial R_{\text{Ir-H}_2}^2} \quad (6)$$

where $\mu_{\text{H-H}}$ and $\mu_{\text{Ir-H}_2}$ are the reduced masses for motion along both axes.

(54) Helgaker, T.; Jaszunski, M.; Ruud, K. *Chem. Rev.* **1999**, *99*, 293–352.

(55) Vaara, J.; Jokisaari, J.; Wasylishen, R. E.; Bryce, D. L. *Prog. Nucl. Magn. Reson. Spectrosc.* **2002**, *41*, 233–304.

Table 1. Vibrational Energy Levels for the HH Isotopomer of Complex **2** and Expectation Values for the Geometrical Parameters of the M–H₂ Unit^a

| ν | E_ν (kcal/mol) | $\langle R_{H-H} \rangle$ (Å) | $\langle R_{Ir-H_2} \rangle$ (Å) |
|-------|--------------------|-------------------------------|----------------------------------|
| 0 | 4.04 | 1.60 | 1.39 |
| 1 | 5.34 | 1.18 | 1.56 |
| 2 | 6.53 | 1.42 | 1.48 |
| 3 | 8.15 | 1.36 | 1.52 |
| 4 | 9.65 | 1.31 | 1.56 |
| 5 | 9.95 | 1.59 | 1.42 |
| 6 | 11.23 | 1.35 | 1.55 |
| 7 | 11.51 | 1.35 | 1.52 |
| 8 | 12.88 | 1.31 | 1.59 |
| 9 | 13.08 | 1.45 | 1.50 |

^a Only levels within 10 kcal/mol of the ground vibrational state are shown. The zero of the energy scale is the potential energy minimum structure. For comparison purposes, we give the geometric parameters and relative energies of the minima in the potential energy surface. *cis*-Dihydride structure: $R_{H-H} = 1.63$ Å, $R_{Ir-H_2} = 1.37$ Å, $E = 0.00$ kcal/mol; dihydrogen structure: $R_{H-H} = 0.93$ Å, $R_{Ir-H_2} = 1.65$ Å, $E = +1.40$ kcal/mol.

Once the vibrational eigenstates are known, it is possible to determine the expectation values of the geometrical parameters R_{H-H} and R_{Ir-H_2} for selected vibrational states by using the standard procedure in quantum mechanics to extract expectation values from the wave function

$$\langle R_{H-H} \rangle_i = \frac{\langle \chi_i | \hat{R}_{H-H} | \chi_i \rangle}{\langle \chi_i | \chi_i \rangle} \quad (7)$$

and an identical expression for $\langle R_{Ir-H_2} \rangle_i$. $\langle R_{H-H} \rangle_i$ and $\langle R_{Ir-H_2} \rangle_i$ are the values determined for the geometrical parameters R_{H-H} and R_{Ir-H_2} if the system were confined in vibrational eigenstate i . Table 1 shows the energy spectrum of the vibrational Hamiltonian for the HH isotopomer along with the expectation values for the geometrical parameters.

The derived ZPE is substantial (4.04 kcal/mol), much larger than that found using the previous 1D model (0.65 kcal/mol),¹⁷ even though a substantial contribution to the new ZPE comes from motion roughly orthogonal to the coordinate leading from the minima to the transition state structure. This will significantly affect the vibrational eigenfunctions. One can quantitatively assess the consequences of this fact by integrating the probability density for the ground vibrational state over $R_{Ir-H_2} \geq 1.50$ Å, the region conventionally described as “classical dihydride”. This simple computation reveals that only 75.1% of the probability density remains in the dihydride region and that 24.9% of the density leaks out toward areas of configurational space with increasing dihydrogen character. In view of this, it is clear that this complex (in the vibrational ground state) cannot be described as a dihydrogen, but also not as a classical dihydride, for which one would expect the probability density to be confined in the dihydride region. Even though from the electronic structure point of view this complex is a dihydride, because of the substantial dihydrogen character it needs to be distinguished from conventional dihydrides, and we consider it to be a compressed dihydride with mean $R_{H-H} = 1.60$ Å and $R_{Ir-H_2} = 1.39$ Å (at $T = 0$ K).

An anharmonic vibrational analysis on the 2D PES can be used to identify the nature of the vibrational transitions. A similar analysis has been reported previously on complex **1**.⁴⁸ To do this, the vibrational wave functions have been graphically analyzed with regard to the number and type of nodal surfaces, and we have identified that there is a set of two different

excitation series, which can be identified as “normal modes” of vibration of the Ir–H₂ unit in this simplified model. Thus, states $\nu = 1, 2, 3$, and 4 are progressive excitations of a low-energy mode, because the corresponding wave functions show one, two, three, and four nodal surfaces, respectively, approximately parallel to each other. The first excitation of this mode (i.e., excitation $1 \leftarrow 0$) occurs at 457 cm⁻¹. Consecutive excitations of this mode appear neither evenly spaced (as would be the case if the vibration were harmonic) nor with decreasing energy gaps (as would be the case in Morse-like anharmonic potential energy profiles): 416 cm⁻¹ ($2 \leftarrow 1$), 567 cm⁻¹ ($3 \leftarrow 2$), 525 cm⁻¹ ($4 \leftarrow 3$). This irregular progression is because this mode describes mainly motion about a potential energy profile of a nondegenerate double well. State $\nu = 5$, on the other hand, corresponds to the first excitation of a high-energy mode, because it has a nodal surface approximately orthogonal to those of states 1–4. The first excitation of this normal mode (i.e., excitation $5 \leftarrow 0$) occurs at 2069 cm⁻¹. Figure 4 shows the probability density plots of some of these vibrational states.

From the shape of the nodal surfaces in Figure 4, it can be seen that the low-energy mode implies mostly the lengthening of R_{H-H} together with slight shortening of R_{Ir-H_2} , whereas the high-energy mode implies mostly elongation of R_{Ir-H_2} and a slight increase of R_{H-H} . According to these descriptions, the low-energy mode is for the most part an H–H stretch, and the high-energy mode is mostly an Ir–H₂ stretch, in contrast to what could be intuitively expected. A scheme of these motions is depicted in Figure 5.

In a previous study of the elongated dihydrogen complex **1**, the same anharmonicity and extensive mixing of the M–H₂ and H–H stretches was encountered, even though in that case there was a potential energy well in the dihydrogen region only.^{10,48} For complex **1**, the H–H and Ru–H₂ stretches were mixed such that both the high-energy and low-energy modes had a substantial component of H–H stretch. In complex **2**, the mixing is even more extensive: the low-energy mode is the one that has actually most of the H–H stretching character.

For complex **1** it was predicted that different isotopomers of the complex, as far as the H₂ ligand was concerned, would display different geometries of the Ru–H₂ unit.¹⁰ This was due to the different ZPE of the complex depending on its isotopic composition, which, because of the high anharmonicity of the PES, had noticeable effect on the shape of the ground state vibrational wave function, which manifested itself in the form of the heavier isotopomers displaying significantly shorter H–H distances. This prediction was later confirmed experimentally.^{20,21}

We have also determined the ground vibrational energy levels of all six possible isotopomers of complex **2**, along with the expectation values of the geometrical parameters of the Ir–H_AH_B unit, which are collected in Table 2. It can be seen that an isotope effect is to be expected in this case, but that because of the specific shape of the PES with a deeper minimum on the dihydride side, the heavier isotopomers would display longer H–H distances and shorter Ir–H₂ distances to a lesser extent. From Table 2 it is evident that indeed, when the reduced mass of the H₂ unit increases, the ZPE diminishes and $\langle R_{H-H} \rangle$ increases along with a more modest shortening of $\langle R_{Ir-H_2} \rangle$. It would certainly be interesting to see whether this prediction can be experimentally verified, because this would be an

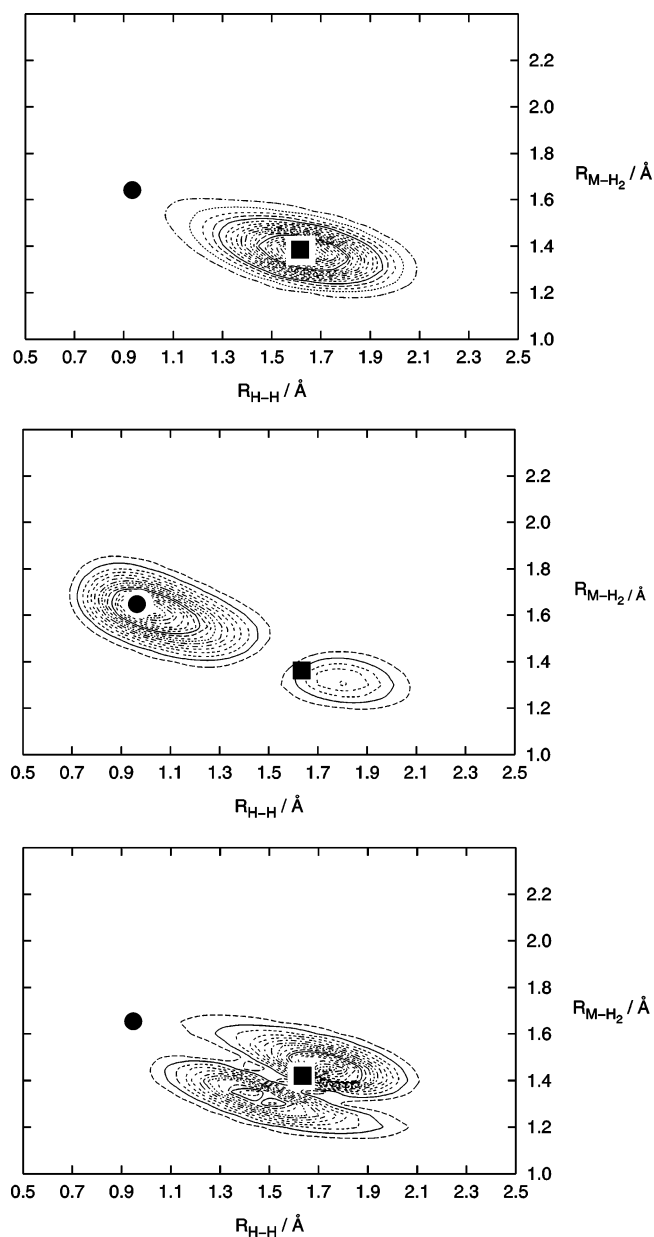


Figure 4. Probability density $|\psi|^2$ for the vibrational ground state (top), first excitation of the low-energy mode ($\nu = 1$, middle), and first excitation of the high-energy mode ($\nu = 5$, bottom). Minima on the potential energy surface are denoted with \bullet (dihydrogen structure) and \blacksquare (*cis*-dihydride structure).

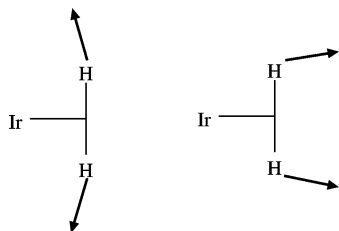


Figure 5. Schematic plot of the atomic motions associated with the low-energy (left) and high-energy (right) modes.

example of distinct experimental behavior that would clearly tell apart elongated dihydrogen and compressed dihydride complexes.

We now turn to the computation of the mean values of $\langle {}^1J_{\text{HD}} \rangle$ for each vibrational level through eq 2 and the temperature

Table 2. Reduced Masses, Zero Point Energies, and Expectation Values of the Geometrical Parameters of the Ir–H₂ Unit in the Ground Vibrational State for the Six Different Isotopomers of Complex 2

| isotopomer | $\mu_{\text{H}_1\text{H}_2}$ (amu) | ZPE (kcal/mol) | $\langle R_{\text{H-H}} \rangle$ (Å) | $\langle R_{\text{M-H}_2} \rangle$ (Å) |
|------------|------------------------------------|----------------|--------------------------------------|----------------------------------------|
| HH | 0.50 | 4.04 | 1.60 | 1.39 |
| HD | 0.67 | 3.39 | 1.62 | 1.38 |
| HT | 0.75 | 3.05 | 1.63 | 1.37 |
| DD | 1.0 | 2.86 | 1.64 | 1.37 |
| DT | 1.2 | 2.58 | 1.64 | 1.37 |
| TT | 1.5 | 2.33 | 1.65 | 1.37 |

Table 3. Vibrational Energy Levels for the HD Isotopomer of Complex 2, Expectation Values for the Geometrical Parameters of the Ir–HD Unit, and State Averaged $\langle {}^1J_{\text{HD}} \rangle$ Values^a

| ν | E_ν (kcal/mol) | $\langle R_{\text{H-D}} \rangle$ (Å) | $\langle R_{\text{Ir-HD}} \rangle$ (Å) | $\langle {}^1J_{\text{HD}} \rangle$ (Hz) |
|-------|--------------------|--------------------------------------|----------------------------------------|------------------------------------------|
| 0 | 3.39 | 1.62 | 1.38 | 6.0 |
| 1 | 4.63 | 1.17 | 1.56 | 22.3 |
| 2 | 5.44 | 1.41 | 1.47 | 15.0 |
| 3 | 6.77 | 1.35 | 1.51 | 17.8 |
| 4 | 7.98 | 1.31 | 1.55 | 20.4 |
| 5 | 8.33 | 1.61 | 1.40 | 6.9 |
| 6 | 9.25 | 1.32 | 1.55 | 20.5 |
| 7 | 9.71 | 1.37 | 1.50 | 16.1 |
| 8 | 10.63 | 1.31 | 1.57 | 21.4 |
| 9 | 10.81 | 1.41 | 1.49 | 16.4 |
| 10 | 11.95 | 1.29 | 1.60 | 22.5 |
| 11 | 12.35 | 1.47 | 1.48 | 15.5 |
| 12 | 13.16 | 1.55 | 1.46 | 10.9 |
| 13 | 13.24 | 1.32 | 1.60 | 21.4 |

^a Only levels within 10 kcal/mol of the ground vibrational state are shown. The zero of the energy scale is the potential energy minimum structure.

dependence of the observed spin–spin coupling constant, through use of eqs 3 and 4, and analogously for the chemical shift. To compute mean $\langle {}^1J_{\text{HD}} \rangle$ values for a specific vibrational state we should apply eq 2, and thus $\langle {}^1J_{\text{HD}} \rangle_i$ depends on the vibrational state, $|\chi_i\rangle$. However, the energy and eigenvector for this state depend on the nature of the isotopes in the Ir–H₂ unit. Although it has been known for a long time that $\langle {}^1J_{\text{HD}} \rangle$ and $R_{\text{H-H}}$ are connected, this is not surprising because we have established on theoretical grounds that $\langle R_{\text{H-H}} \rangle_i$ depends actually on the isotopic composition of the H₂ unit (see Table 2 for complex 2, and refs 20 and 21). We have solved eq 1 again for the HD isotopomer to obtain vibrational states, geometry expectation values (eq 7), and $\langle {}^1J_{\text{HD}} \rangle_i$ (eq 2). The results of this analysis are presented in Table 3.

The main effect of the isotopic substitution (cf. Table 1) is the predictable lowering of the ZPE, which comes along with a denser packing of the vibrational states. As for the geometry expectation parameters, the ground state shows a noticeably longer H–H distance but vibrational excited states do not display a monotonic trend toward shorter or longer distances with respect to the corresponding states in the HH isotopomer. This is because in the H–H direction the potential energy profile can be described as a potential double well. Surprisingly enough, the Ir–HD distances are always shorter than (or equal to) their Ir–HH counterparts, the reason being that in the Ir–H₂ direction the potential energy profile is a single, although anharmonic, potential energy well.

The value of $\langle {}^1J_{\text{HD}} \rangle_{\nu=0} = 6.0$ Hz corresponds to what would be measured at $T = 0$ K for the spin–spin coupling constant. This value differs from that of the precise structure at the potential energy minimum and is nonetheless closer to the range of values experimentally determined. The difference is inter-

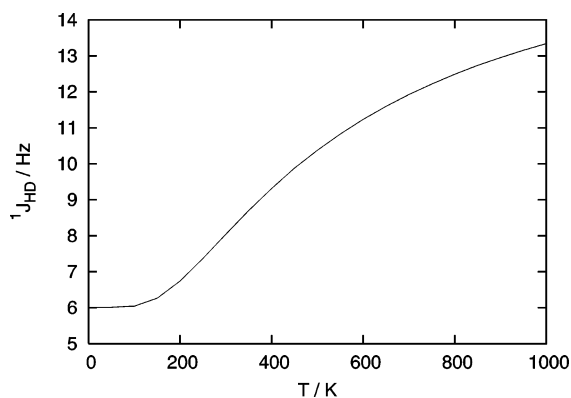


Figure 6. Thermal average over vibrational states of the spin–spin coupling constant, $^1J_{HD}(T)$, for the HD isotopomer. The dynamical model does not describe the dissociation of the complex at sufficiently high temperature. The complex is stable over hours at room temperature (300 K). It has not been heated beyond room temperature, where it is reasonably stable.

preted taking into account that $\langle ^1J_{HD} \rangle_{v=0}$ corresponds to the averaged value of $^1J_{HD}(R_{H-D}, R_{Ir-HD})$ using $|\psi_{v=0}|^2$ for the HD isotopomer (HD equivalent of Figure 4, top) as a weighting function, which also has an important amplitude all over the range of R_{H-D} distances from 1.3 to 2.0 Å. Actually, the value of $\langle ^1J_{HD} \rangle_i$ is greatly influenced by the shape of the probability density of state i : for instance the first excited vibrational state has a very large amplitude in a region of short H–H distances where $^1J_{HD}(R_{H-D}, R_{Ir-HD})$ takes on large values, and as a consequence, $\langle ^1J_{HD} \rangle_{v=1}$ is very large (22.3 Hz).

The $\langle ^1J_{HD} \rangle_i$ values shown in Table 3 are specific to vibrational state i and do not correspond to what is to be measured in the NMR experiments (with the only possible exception of the value for the ground state, previously discussed). The thermal average, $^1J_{HD}(T)$, is obtained through use of eqs 3 and 4 and is depicted in Figure 6. To our knowledge, this is the first time that a first-principles determination of the temperature dependence of the $^1J_{HD}$ coupling constant has been carried out for an elongated dihydrogen or compressed dihydride complex.

Figure 6 predicts an increase of $^1J_{HD}$ with T , in complete agreement with experimental findings. Because this behavior has been predicted without resorting to any correlation between $^1J_{HD}$ and R_{H-H} , we think that this strongly supports the hypothesis that the thermal dependence of $^1J_{HD}$ in elongated dihydrogen complexes (and compressed dihydride complexes) is due to the extreme anharmonicity of the potential energy surface describing the motion of the $M-H_2$ unit.

Our theoretical results agree reasonably well with reported experimental data. At $T = 223$ K theory predicts $^1J_{HD} = 7.0$ Hz, which compares very well to an experimental measurement of $^1J_{HD} = 7.3$ Hz, and at $T = 303$ K theory predicts $^1J_{HD} = 8.1$ Hz, which compares satisfactorily to experiment (9.0 Hz).¹⁹ We want to highlight that quantitative agreement in the temperature dependence of $^1J_{HD}$ is difficult to achieve, because it depends strongly on the precision to which vibrational states (both wave functions and energies) are determined, due to the exponential dependence in the Boltzmann average. Our treatment of this problem is qualitatively correct and sophisticated, but is only 2D. Inclusion of other degrees of freedom, if possible, would increase enormously the number of vibrational states, making it easier to populate excited states. Presumably then, inclusion of further degrees of freedom would make the temperature dependence of $^1J_{HD}$ more steep and closer to experiment than

Table 4. Vibrational State Averaged Values of the Chemical Shift δ for Isotopomers HH and HD^a

| v | $\langle \delta_{HH} \rangle$ (ppm) | $\langle \delta_{HD} \rangle$ (ppm) |
|-----|-------------------------------------|-------------------------------------|
| 0 | −3.805 | −3.893 |
| 1 | −2.939 | −2.957 |
| 2 | −3.336 | −3.409 |
| 3 | −3.063 | −3.171 |
| 4 | −2.798 | −2.942 |
| 5 | −3.355 | −3.551 |
| 6 | −2.803 | −2.866 |
| 7 | −2.824 | −3.000 |
| 8 | −2.465 | −2.721 |
| 9 | −2.949 | −3.042 |
| 10 | | −2.475 |
| 11 | | −3.041 |
| 12 | | −2.993 |
| 13 | | −2.392 |

^a Only values for states within 10 kcal/mol of the respective ground state are shown. For energy levels, see Tables 1 and 3.

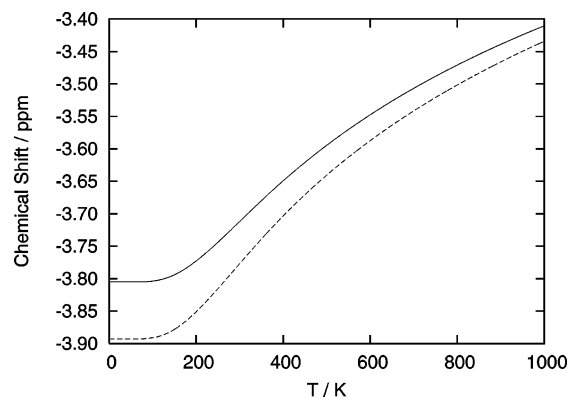


Figure 7. Temperature dependence of the chemical shifts for the HH (solid line) and HD (dashed line) isotopomers of **2**. See caption of Figure 6 for thermal stability of complex **2**.

it is now because the first excitation of the low-energy mode populates a state with very large $\langle ^1J_{HD} \rangle_i$.

Finally, we focus on the computation of the temperature dependence of the proton chemical shift. The isotope effect on the chemical shift at a given temperature T , $\Delta\delta(T)$, is given by

$$\Delta\delta(T) = \delta_{HD}(T) - \delta_{HH}(T) \quad (8)$$

To determine the temperature dependence of the chemical shifts of both isotopomers, $\langle \delta_{HH} \rangle_i$ and $\langle \delta_{HD} \rangle_i$, the state averaged values of the chemical shift for both isotopomers need to be computed. These are gathered in Table 4.

First, focusing on the HH isotopomer, it is worthwhile noting that in general there is a correlation between $\langle R_{Ir-H_2} \rangle_i$ and $\langle \delta_{HH} \rangle_i$, such that the shorter the former is, the further toward higher field (i.e., toward negative δ values) the latter appears (see Tables 1 and 3). Again this agrees with the usual interpretation that higher electron density on a given nucleus means stronger shielding. The same behavior is observed for the HD isotopomer.

$\langle \delta_{HD} \rangle_i$ appears at higher field than $\langle \delta_{HH} \rangle_i$. This is a consequence of the isotopic geometric effect predicted previously (cf. Tables 1 and 3), by virtue of which heavier isotopic substitutions lead to shorter Ir–H₂ distances for each vibrational state. The temperature dependence of the chemical shifts for both isotopomers are readily computed through a Boltzmann average (Figure 7). Despite the fact that absolute values of the chemical shifts are far from experimental values, we focus now on the

trends displayed by $\Delta\delta(T)$. First and foremost, $\delta_{\text{HH}}(T)$ is above $\delta_{\text{HD}}(T)$ for the complete range of temperatures, meaning that the isotope effect on the chemical shift as defined in eq 8 is *negative*, that is, to higher field, in agreement with experiment. In Figure 7 the isotope effect is incidentally only the distance between both curves at a given temperature. Thus, it is possible to see that on decreasing temperature we predict a *larger* isotope effect, also in complete agreement with experiment. For the sake of comparison, we give the explicit theoretical values at the same temperatures at which experimental data are available: $\Delta\delta$ (223 K) = -75 ppb (experimental value is -134 ppb) and $\Delta\delta$ (303 K) = -64 ppb (experimental value is -91 ppb). We think that the agreement is quite good, especially taking into account the strong (exponential) dependence of these values on the energy of the vibrational states and the shape of the vibrational wave functions, as previously commented.

In summary, there is good agreement between experiment and theoretical predictions in strong support of the validity of our model and the theoretical treatment. It seems reasonable to conclude that the anharmonicity of the potential energy surface, with a deeper minimum in the dihydride region, and the effects it has on the vibrational states of the Ir-H₂ unit, is likely to be the cause of the odd properties of complex **2**, and that the physics behind its properties is hence correctly accounted for once the delocalization of the nuclear wave function is explicitly considered.

4. Conclusions

A complete electronic structure + nuclear dynamics study has been done on complex [Cp*Ir(dmppm)H₂]²⁺ to determine the temperature dependence of ¹J_{HD}, solely on theoretical grounds. A complete 2D PES for this complex has been built using density functional theory and found to be very anharmonic as seems to be the norm in the so-called stretched dihydrogen/compressed dihydride complexes.

Vibrational energy levels and wave functions have been calculated for different isotopomers of the Ir-H₂ unit. The results point in the direction that for the ground vibrational state a geometrical isotope effect is to be expected, such that heavier isotopic substitutions would bring about *longer* H-H distances. This behavior is exactly the opposite of that first predicted by us for elongated dihydrogen complex [Cp*Ru(dppm)(H₂)⁺ and

later verified experimentally. This behavior could be an essential feature of compressed dihydride complexes.

A detailed anharmonic vibrational analysis has been performed on the Ir-H₂ unit of the complex, and it has been found that the H-H stretch is actually a low-frequency motion, and the Ir-H₂ stretch corresponds to a high-frequency motion in this complex.

A complete 2D surface for ¹J_{HD} as a function of the geometry of the Ir-H₂ unit has been computed. In this way, it has been found that ¹J_{HD} depends, as is well-known, not only on the H-D distance, but also on the Ir-HD distance. The preceding results have been used to compute vibrational state averaged values of ¹J_{HD} and, using a Boltzmann average, the temperature-dependent spin-spin coupling constant. The latter is found to be in good agreement with experiment.

The chemical shift as a function of the geometry of the Ir-H₂ unit has also been computed. The values of the chemical shift are far from the experimental range. However, when used to compute state averaged chemical shift values, the isotope effect on the chemical shift as a function of temperature is correctly and satisfactorily reproduced.

The ability to reproduce almost quantitatively ¹J_{HD} as a function of temperature and obtain a qualitative agreement on the temperature dependence of the isotope effect on the chemical shift validate the methodology used and provide support for the hypothesis that the strange properties of complex **2** in particular, and elongated dihydrogen and compressed dihydride complexes in general, stem from the important anharmonicity of the potential energy surface describing the motion of the M-H₂ unit and the effects this has on the vibrational energy levels and wave functions.

Acknowledgment. R.G. acknowledges the Spanish “Ministerio de Ciencia y Tecnología” for a “Ramón y Cajal” research contract. We are grateful for financial support from the Spanish “Ministerio de Ciencia y Tecnología” and the “Fondo Europeo de Desarrollo Regional” through projects BQU2002-00301 and BQU-2002-04110-C02-02. The use of computational facilities at the “Centre de Supercomputació de Catalunya” is gratefully acknowledged. D.M.H. acknowledges support from the U.S. National Science Foundation.

JA043011R